BMC Biology

RESEARCH ARTICLE

Open Access

The *mrp-3* gene is involved in haem efflux and detoxification in a blood-feeding nematode

Danni Tong[1†], Fei Wu[1†], Xueqiu Chen[1], Zhendong Du[1], Jingru Zhou[1,2], Jingju Zhang[1], Yi Yang[1], Aifang Du[1] and Guangxu Ma[1*]

Abstract

Background Haem is essential but toxic for metazoan organisms. Auxotrophic nematodes can acquire sufficient haem from the environment or their hosts in the meanwhile eliminate or detoxify excessive haem through tightly controlled machinery. In previous work, we reported a role of the unique transporter protein HRG-1 in the haem acquisition and homeostasis of parasitic nematodes. However, little is known about the haem efflux and detoxification via ABC transporters, particularly the multiple drug resistance proteins (MRPs).

Results Here, we further elucidate that a member of the *mrp* family (*mrp-3*) is involved in haem efflux and detoxification in a blood-feeding model gastrointestinal parasite, *Haemonchus contortus*. This gene is haem-responsive and dominantly expressed in the intestine and inner membrane of the hypodermis of this parasite. RNA interference of *mrp-3* resulted in a disturbance of genes (e.g. *hrg-1*, *hrg-2* and *gst-1*) that are known to be involved in haem homeostasis and an increased formation of haemozoin in the treated larvae and lethality in vitro, particularly when exposed to exogenous haem. Notably, the nuclear hormone receptor NHR-14 appears to be associated the regulation of *mrp-3* expression for haem homeostasis and detoxification. Gene knockdown of *nhr-14* and/or *mrp-3* increases the sensitivity of treated larvae to exogenous haem and consequently a high death rate (> 80%).

Conclusions These findings demonstrate that MRP-3 and the associated molecules are essential for haematophagous nematodes, suggesting novel intervention targets for these pathogens in humans and animals.

Keywords Haematophagous nematodes, *Mrp*, Haem efflux, Haem detoxification, Target candidate

Background

Haem (iron-protoporphyrin IX) is a requisite for a range of biological reactions, including oxygen transfer, oxidative metabolism, photosynthesis, and signal transduction [1, 2]. However, free haem is a potent pro-oxidant and pro-inflammatory molecule [3], and as a hydrophobic molecule, it can intercalate into the phospholipid bilayer of cell membranes and bind to proteins, leading to biomolecular structure disruption [4]. Multiple haem detoxification mechanisms have been reported in all life forms, including protozoa, fungi, arthropods, and mammals [3, 5–8], which usually involve haem sequestering [9–12] and degradation [13, 14].

Roundworms (nematodes) are haem auxotrophs that are entirely reliant on exogenous haem from the environment or host animals [15, 16]. It is interesting to know how nematodes acquire exogenous haem and limit the toxicity of haem [1]. Over the past 20 years, a growing number of proteins involved in haem acquisition, trafficking, and detoxification have been reported in a free-living

†Danni Tong and Fei Wu contributed equally to this work.

*Correspondence:
Guangxu Ma
gxma1@zju.edu.cn
[1] Institute of Preventive Veterinary Medicine, Zhejiang Provincial Key Laboratory of Preventive Veterinary Medicine, College of Animal Sciences, Zhejiang University, Hangzhou 310058, Zhejiang, China
[2] MOE Frontier Science Center for Brain Science and Brain-Machine Integration, Zhejiang University, Hangzhou 311121, Zhejiang, China

nematode *Caenorhabditis elegans*, the best-studied metazoan model organism [17–22]. In this free-living nematode, a series of haem responsive genes (*hrg*) have been identified to play roles in haem acquisition (e.g. *hrg-4*, *-5*, and *-6*) from the environment, haem mobilising from the intestine (e.g. *hrg-1*, *-9*, and *-10*) then to other tissues (e.g. *hrg-2* and *hrg-3*), and haem homeostasis (e.g. *hrg-2* and *hrg-7*) [17, 18, 20–25]. Although similar haem acquisition and homeostasis machinery (e.g. haem responsive feature for HRG-1) have been proposed in parasitic nematodes [26, 27], little is known about the detailed mechanisms underlying haem detoxification, except for haemozoin formation, a crystallised form of oxidised haem [28, 29].

In addition to a negative feedback regulation of haem acquisition [27], there might be complementary haem efflux machinery in parasitic nematodes. ATP-binding cassette (ABC) transporters, particularly the ABCC family, also known as multiple drug resistance proteins (MRPs), have been proposed to play a role in haem export [19, 30, 31]. For instance, MRP-5 has been demonstrated to transport haem across the basolateral membrane of the intestine into the pseudocoelom of *C. elegans* [19], and gene silencing of the *mrp-5* homologue in *Drosophila melanogaster* resulted in haem accumulation in the intestine and lethality [31]. However, almost nothing is known about haem exporter and its roles in haem detoxification in parasitic nematodes, particularly blood-feeding species, which ingest a great deal of host blood but are capable of coping with the free haem released from ruptured red blood cells. Here, we screened members of the *mrp* gene family that are haem-responsive and required for haem efflux and detoxification in *Haemonchus contortus*, a model gastrointestinal nematode [32], and demonstrated how the key members work and are regulated in this blood-feeding parasite.

Results

mrp-3 gene is more sensitive to exogenous haem in a blood-feeding nematode

Genome-wide screening identified six genes (i.e. HCON_00189480, HCON_00009950, HCON_00175410, HCON_00164880, HCON_00144960, and HCON_00110560) coding for MRPs in *H. contortus*, a blood-feeding model of gastrointestinal nematode, in which these genes were predicted as orthologues to *mrp-1/2*, *mrp-3*, *mrp-4*, *mrp-5*, *mrp-6*, and *mrp-7* of the free-living model organism *C. elegans*, respectively (Fig. 1a). The orthologue of *mrp*-8 was not predicted in *H. contortus*. A similar number of *mrp* gene orthologues were also predicted in other parasitic nematodes, including *Ancylostoma caninum*, *Angiostrongylus cantonensis*, and *Nippostrongylus brasiliensis*, which are all blood-feeding worms (Additional file 1: Table S1). By exploiting previous transcriptomic data sets available for *H. contortus*, we found that the transcriptional levels of most *mrp* genes were low (fragments per kilobase million, FPKM < 100), but tightly regulated during the life history (i.e. the egg, first larval stage L1, second larval stage L2, third larval stage L3, fourth larval stage L4, and adult), particularly during the transition from free-living (i.e. the infective L3) to parasitic (L4) stage (Fig. 1b).

By exposing the free-living second-stage larvae (L2s, which feed on bacteria in the environment) and blood-feeding adults (a mix of females and males) of *H. contortus* to 10 μM of haemin chloride in vitro, we detected transcriptional alterations of *Hc-mrp-1/2*, *Hc-mrp-3*, *Hc-mrp-4*, *Hc-mrp-5*, *Hc-mrp-6*, and *Hc-mrp-7* genes in the treated worms, compared with untreated worms (Fig. 1c and 1d). A higher initial concentration (100 μM) of haemin chloride even increased or decreased the transcriptional alterations of these genes in either L2s or adults of *H. contortus* (Fig. 1c and 1d). Notably, 10 or 100 μM of haemin chloride treatment consistently resulted in a significant downregulation of *Hc-mrp-3* in both L2s ($P < 0.01$) and adults ($P < 0.001$) of *H. contortus*, compared with untreated control (Fig. 1c and 1d), in accord with the haem response of *hrg-1* in this nematode [27].

MRP-3 protein appears to play a role in haem export in vitro and in vivo

By constructing a lentivirus-transduced mammalian cell line (HEK 293 T) that stably expresses *Hc*-MRP-3-GFP, this protein was found predominant in the cytoplasm in cells (Additional file 2: Fig.S1, right panel), partially co-localised with endosomes and lysosomes, and distributed on plasma membrane based on the location of markers hRab5a, hRab7a, Lyso-Tracker, and Dil, respectively (Fig. 2a). We also tested the role of *Hc*-MRP-3-FLAG in haem transport using a fluorescence efflux assay (Additional file 2: Fig.S1). Compared with wild-type and irrelative (rhodamine 123, a fluorescent substrate of the P-glycoprotein multidrug transporter) controls, a significant ($P < 0.001$) lower intensity of either calcein or carboxyfluorescein (CF) fluorescence was detected in the cells expressing *Hc*-MRP-3 (Fig. 2b). In contrast, the increased fluorescence efflux efficiency due to *Hc*-MRP-3 overexpression was significantly ($P < 0.001$) suppressed after treatment with the MRP inhibitor MK571 (Fig. 2c) [33]. These results validate a fluorescent substrate efflux cell line (i.e. *Hc*-MRP-3-expressing HEK 293 T cells). We further incubated these cells with a fluorescent haem analogue (zinc mesoporphyrin IX, ZnMP) [31, 34], in which a significant ($P < 0.001$) lower intensity of fluorescence was detected after 2 h of incubation, compared with a wild-type control (Fig. 2d).

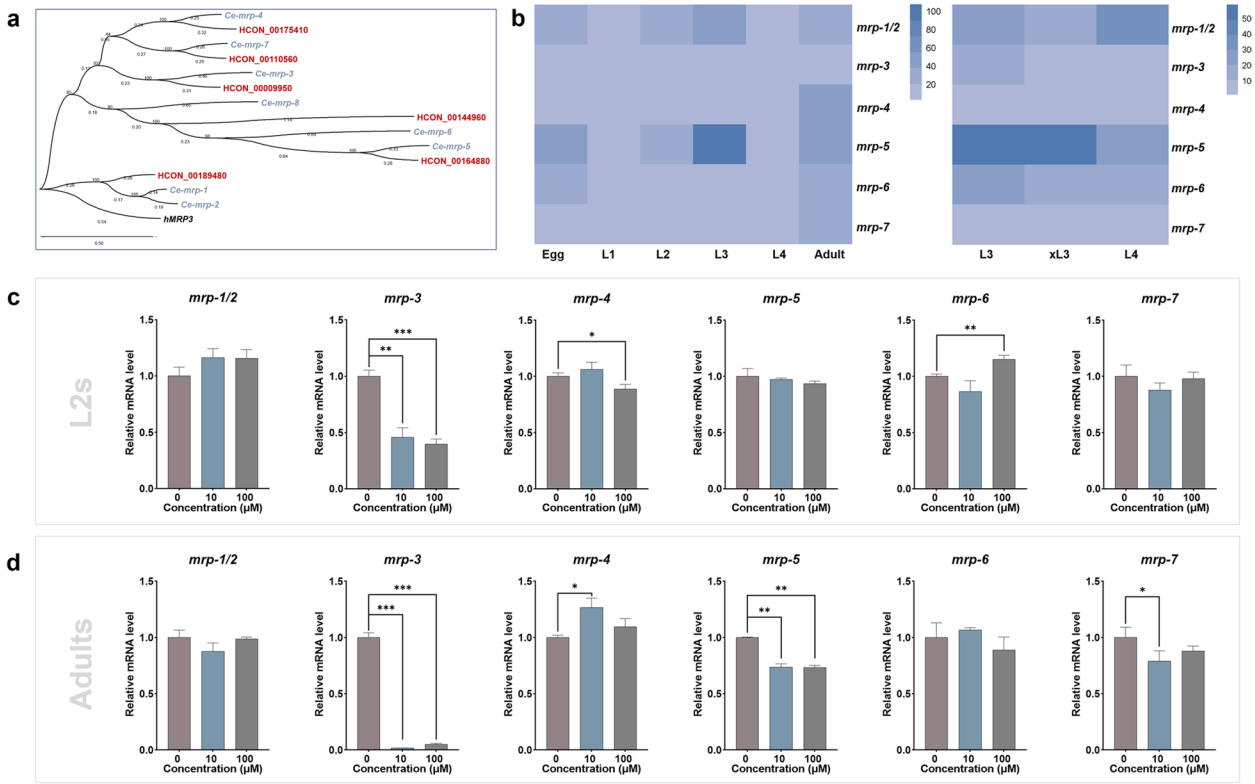

Fig. 1 Screening of haem-responsive *mrp* genes in *Haemonchus contortus*. **a** Phylogenetic analysis of genome widely identified multiple drug resistance proteins (MRP) in*H. contortus* and their homologues in *Caenorhabditis elegans*. Amino acid sequences are aligned using ClustalW and the tree is generated using the Maximum Likelihood method and JTT matrix-based model in MEGA X. Human MRP3 (h*MRP3*) was used as an outgroup. The scale and percentage of trees in which the associated taxa clustered together are shown. **b** Transcriptional profiles of *mrp-1/2*, *-3*, *-4*,*-5*, *-6* and *-7* genes among egg, the first- (L1), second- (L2), third- (L3), fourth-larval (L4) and adult stages of *H. contortus*, and among L3, exsheathed L3 (xL3), in vitro cultured L4 stages of this parasitic nematode. The data is presented as normalised transcripts per million. Transcription of *mrp-1/2*, *-3*, *-4*,*-5*, *-6* and *-7* genes in L2 (c) and adult stages (**d**) of *H. contortus* when exposed to 0, 10 and 100 μM of haemin chloride in vitro. A $2^{-\Delta\Delta CT}$ method is used for relative mRNA level calculation. Data are shown as mean ± standard deviation (SD). Student's *t* test is performed for statistical analyses. **P* < 0.05, ***P* < 0.01, ****P*< 0.001

We tested the potential role of *Hc*-MRP-3 in haem export on a *hem1* mutant of yeast (*Δhem1*) [27], which cannot synthesise δ-aminolevulinic acid (ALA, the first compound in haem synthesis) and consequently cannot grow due to insufficient haem acquisition [35, 36]. By introducing *Ce-hrg-4* (a membrane haem importer coding gene from *C. elegans*) [20] into the *Δhem1*, the mutant grew well on the plate when provided with an initial concertation of 1.0 μM of haemin chloride (Fig. 3a). In contrast, heterologous expression of *Hc*-MRP-3 did not rescue but increased the growth defect of *Δhem1*, even though provided with exogenous haem (Fig. 3a). Protein expression of *Hc*-MRP-3 in the *Δhem1* also compromised the growth of yeast on culture plate and in culture medium supplemented with 250 μM of ALA for endogenous haem biosynthesis in the yeast (Fig. 3b and c), suggesting an efficient export of synthesised haem. The heterologous expression of *Ce*-HRG-4 and *Hc*-MRP-3 in *Δhem1* was confirmed using an indirect immunofluorescent assay (Fig. 3d).

MRP-3 protein is dominant in nematode intestine and hypodermal membrane

To further understand the role of MRP-3 in haem export in nematodes, we first unveiled the tissue distribution of this protein in the blood-feeding nematode *H. contortus*. Using a polyclonal antibodies-based indirect immunofluorescence assay, we found that *Hc*-MRP-3 was dominant in the intestine and the inner hypodermal membrane of adult worms, irrespective of sex (female and male; Additional file 2: Fig.S2a and S2b). This tissue expression pattern of *Hc*-MRP-3 is like that of HRG-1 and HRG-2 proteins in *H. contortus*, which has been reported to play distinct roles in haem homeostasis (haem acquisition and possibly trafficking) of this blood-feeding parasite (Additional file 2: Fig.S2c) [26, 27]. Although *Hc*-MRP-3 was also detected to be dominant in the germ cells of

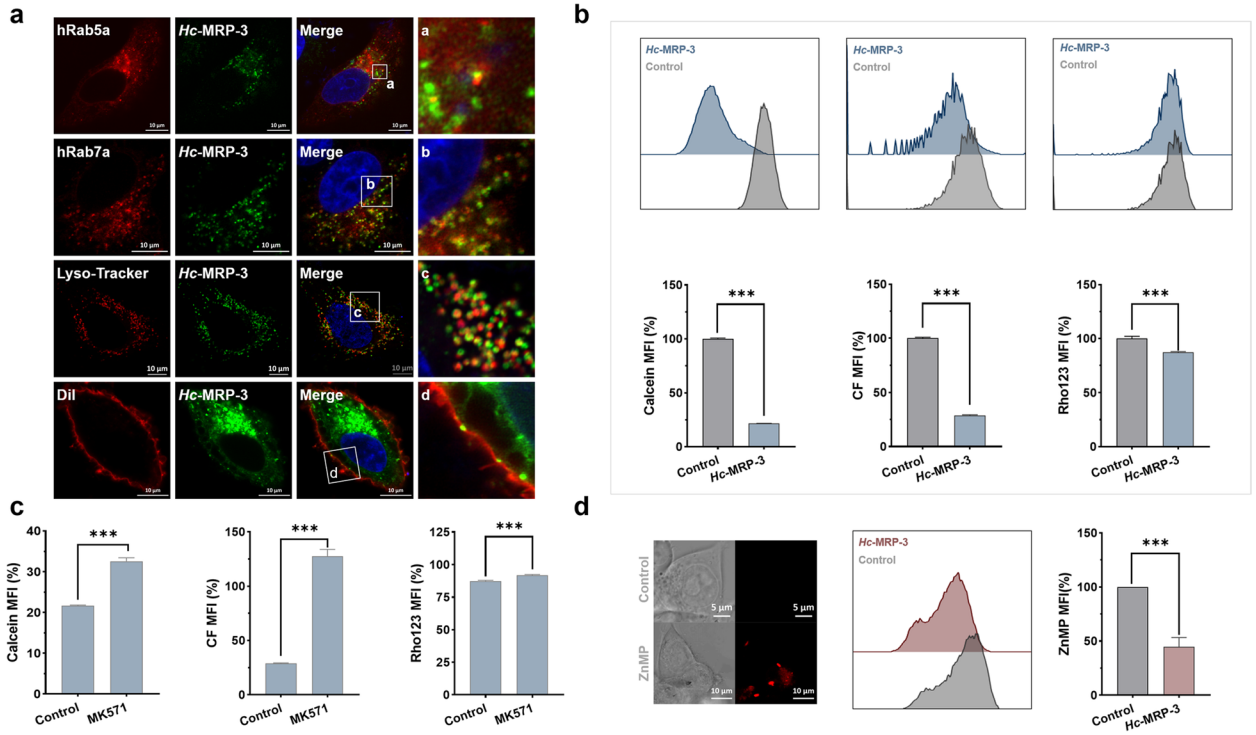

Fig. 2 The exporter activity of *Hc*-MRP-3 in mammalian cells. **a** Co-localisation analysis of *Hc*-MRP-3-green fluorescent protein (GFP) in Hela cells. hRab5a is an early endosomes marker, hRab7a is a late endosomes marker. hRab5a and hRab7a are labeled by mCherry. Lyso-Tracker is a lysosomes marker, and DiI is for plasma staining. DAPI is for nucleus staining. Scale bar, 10 μm as indicated. **b** Calcein, carboxyfluorescein (CF), and Rho123 fluorescence-activated cell sorting (up subpanel) and efflux analyses of cells expressing *Hc*-MRP-3 (down subpanel). **c** Mean fluorescence intensity of calcein, CF and Rho123 in cells expressing *Hc*-MRP-3 after treatment with an MRP inhibitor MK571. **d** Uptake of zinc mesoporphyrin IX (ZnMP; a fluorescent haem analogue) by HEK 293T cells (left subpanel), and fluorescence-activated sorting (middle subpanel) and efflux analysis of cells expressing *Hc*-MRP-3 (right subpanel). Data are shown as mean ± standard deviation (SD). Student's *t* test is performed for statistical analyses. ***$P < 0.001$. MFI, mean fluorescence intensity

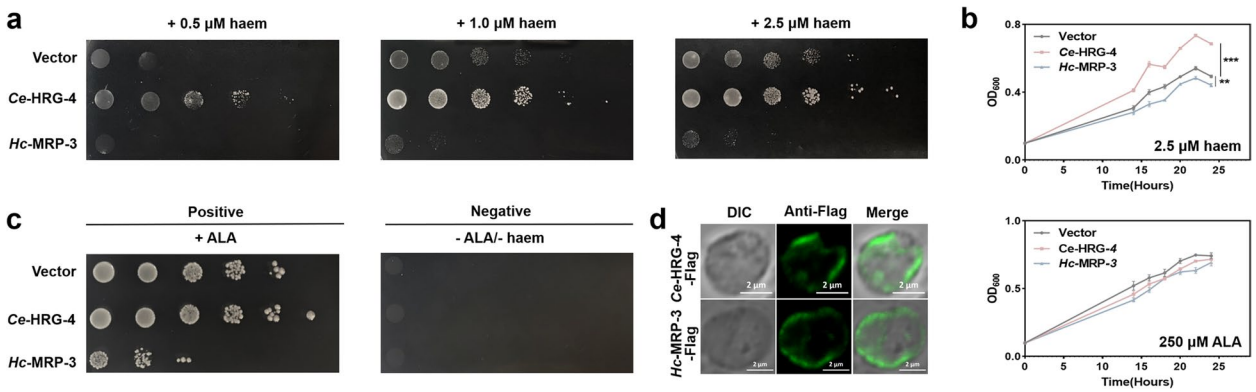

Fig. 3 Haem export activity of *Hc*-MRP-3 in yeast cells. **a** Spotting assay of *Δhem1* (vector control, which cannot synthesise δ-aminolevulinic acid (ALA, the first compound of haem synthesis de novo), *Δhem1* expressing*Ce*-HRG-4 (positive control) or *Hc*-MRP-3 on plate, when supplemented with 0.5, 1.0 or 2.5 μM haemin chloride. **b** Growth assay of *Δhem1* (vector control), *Δhem1* expressing *Ce*-HRG-4 (positive control) or *Hc*-MRP-3 in culture medium, when supplemented with 2.5 μM haemin chloride or 250 μM ALA. The growth of yeast is assessed by measuring $OD_{600}$of the culture medium after 24 h of incubation. **c** Spotting assay of *Δhem1* and *Δhem1* expressing *Ce*-HRG-4 or *Hc*-MRP-3 on plate, when supplemented with ALA. Neither ALA nor haemin chloride is supplemented in the negative control. Data are shown as mean ± standard deviation (SD). Student's *t* test is performed for statistical analyses. **$P < 0.01$, ***$P < 0.001$. **d** Indirect immunofluorescence microscopy of *Δhem1* yeast expressing *Ce*-HRG-4-Flag or *Hc*-MRP-3-Flag using an anti-Flag antibody. Scale bar, 2 μm

H. contortus adult females (Additional file 2: Fig.S2a), suggesting a role of this haem exporter protein during fertilisation and/or embryonation. However, due to technical limitations in exploring these in vivo processes, we focused our study on the role of *Hc*-MRP-3 in the larval and adult stages of *H. contortus*, which can be maintained shortly in vitro.

RNAi(*mrp-3*) compromises the efflux of a fluorescent haem analogue in the free-living larvae

By integrating RNA interference (RNAi)-mediated gene knockdown and fluorescence efflux assays, we tested the role of *Hc-mrp-3* in the free-living larvae (e.g. L1s, L2s, and L3s) of *H. contortus*, in which the transcription of this gene was certainly detected using a quantitative real-time polymerase chain reaction (Additional file 2: Fig. S3a). After efficient gene knockdown of *Hc-mrp-3* ($P < 0.001$; Additional file 2: Fig. S3b), a significant ($P < 0.01$) but not obvious decrease of Rho123 efflux was observed in the treated larvae (Fig. 4c). By contrast, only a punctate distribution in the intestine and regional distribution of calcein and CF were observed in the pharynges of RNAi(*Hc-mrp-3*)-treated larvae of *H. contortus* (Fig. 4a and b), representing significantly decreased efflux rates of calcein (by ~ 40%; $P < 0.001$) and CF (by ~ 40%; $P < 0.001$), compared with untreated and irrelative controls.

Using this RNAi(*Hc-mrp-3*)-treated larval model, we tested the role of MRP-3 in haem export in *H. contortus*. After supplementation with a fluorescent haem analogue ZnMP for 4 h, we detected an accumulation of red fluorescence in the intestine of RNAi(*Hc-mrp-3*)-treated larvae, compared with untreated control (Fig. 4d). However, the impact (a decrease of 25%; $P < 0.05$) of RNAi(*Hc-mrp-3*) on the efflux of ZnMP in treated larvae was not as obvious as that of calcein and CF (a decrease of ~ 40%) (Fig. 4a, b, and d).

mrp-3 gene is involved in haem homeostasis in the free-living larvae

Indeed, compared with wildtype control, gene silencing of *Hc-mrp-3* was linked to increased mRNA levels of *Hc-hrg-1* ($P < 0.001$), *Hc-hrg-2* ($P < 0.01$), and *Hc-gst-1* ($P < 0.001$) in the treated larvae of *H. contortus* (Fig. 5a–c), which all have been reported or proposed to be involved in haem homeostasis [26, 27, 37]. Specifically, when the RNAi-treated larvae were exposed to 0.1 μM of haemin chloride, the transcriptional level of *Hc-hrg-1* ($P < 0.001$), *Hc-hrg-2* ($P < 0.01$), and *Hc-gst-1* ($P < 0.001$) significantly decreased, compared with unexposed larvae (Fig. 5d–f); when the RNAi-treated larvae were exposed to a higher initial concentration (10 μM) of haemin chloride, the transcriptional levels of *Hc-hrg-1* ($P < 0.001$) and *Hc-gst-1* ($P < 0.001$) consistently decreased while the transcriptional level of *Hc-hrg-2* ($P < 0.001$) increased, compared with unexposed larvae or larvae exposed to a lower concentration (0.1 μM) of haem (Fig. 5g–i), indicating a regulatory network of *Hc-mrp-3* and genes involved in haem homeostasis. In addition, an increased level of haemozoin (a crystallisation complex of free haem usually formed during haem detoxification) [7] was detected in the RNAi(*Hc-mrp-3*)-treated larvae of *H. contortus*, particularly when supplemented with 10 μM ($P < 0.001$), 100 μM ($P < 0.05$), and 1000 μM of exogenous haem in the culture medium after either 24, 48 or 72 h (Fig. 5j and k). The relationship among *Hc-mrp-3*, exogenous haem and haemozoin in the free-living larvae of *H. contortus*

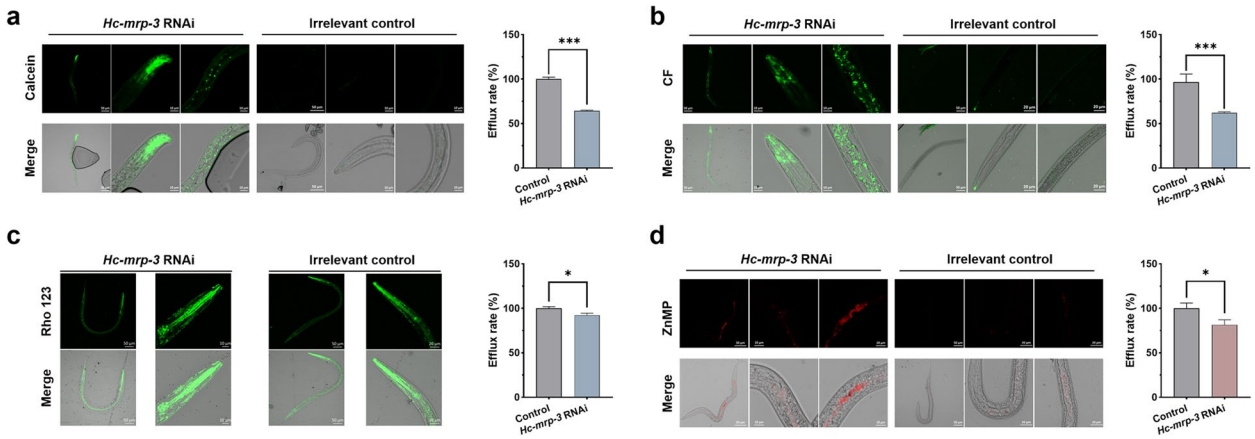

Fig. 4 RNA interference-mediated gene knockdown of *Hc-mrp-3* results in dye accumulation in the gut and pharynx. **a–d** The influences of RNAi(*Hc-mrp-3*) on the efflux of rhodamine 123 (Rho123), calcein, carboxyfluorescein (CF) and zinc mesoporphyrin IX (ZnMP; a fluorescent haem analogue). Data are shown as mean ± standard deviation (SD). Student's *t* test is performed for statistical analyses. Scale bars, 10, or 20 or 50 μm. Data are shown as mean ± standard deviation (SD). Student's *t* test is performed for statistical analyses. *$P < 0.05$, ***$P < 0.001$

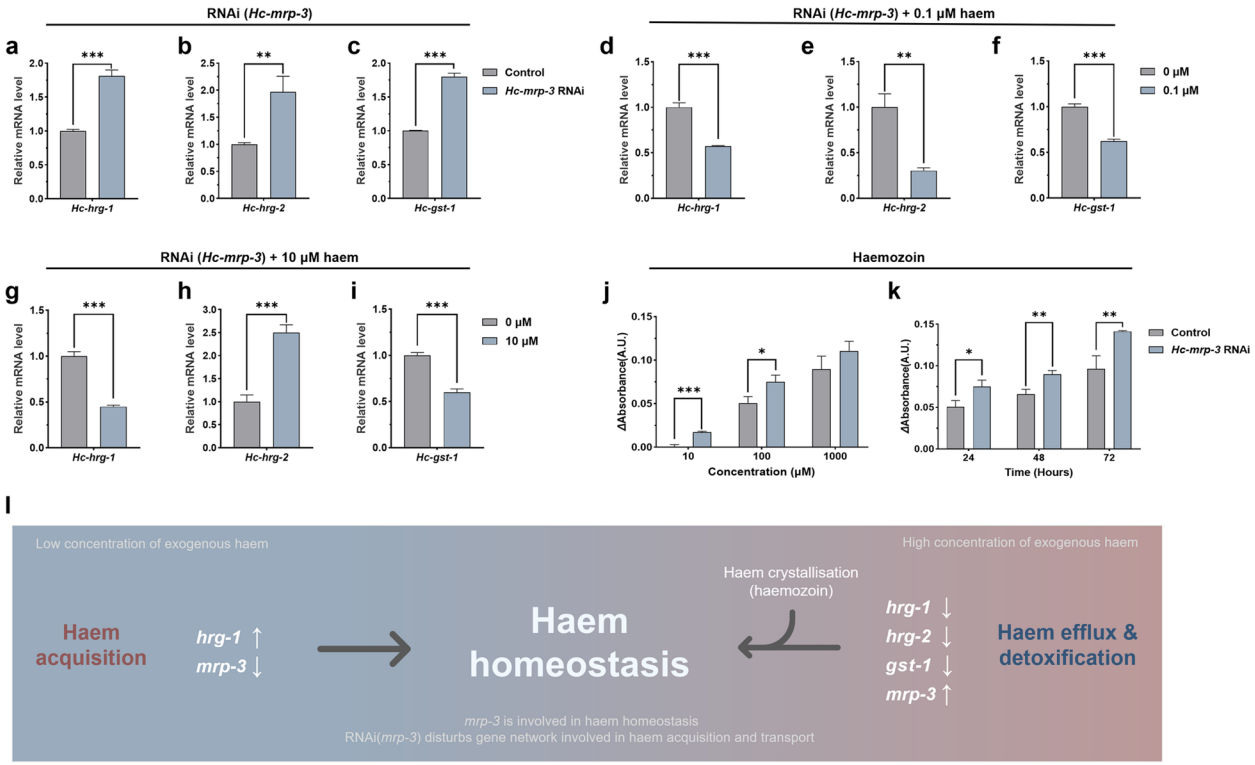

Fig. 5 The involvement of *Hc-mrp-3* in the haem homeostasis of *Haemonchus contortus*. **a–c** Transcriptional alterations of *Hc-hrg-1*, *Hc-hrg-2* and *Hc-gst-1* in the RNAi(*Hc-mrp-3*)-treated exsheathed third-stage larvae (xL3s) of *H. contortus* for 48 h. **d–f** Transcriptional alterations of *Hc-hrg-1*, *Hc-hrg-2* and *Hc-gst-1* in the RNAi(*Hc-mrp-3*)-treated xL3s of *H. contortus* after exposure to 0.1 μM haemin chloride for 24 h. **g–i** Transcriptional alterations of *Hc-hrg-1*, *Hc-hrg-2* and *Hc-gst-1* in the RNAi(*Hc-mrp-3*)-treated xL3s of *H. contortus* after being exposed to 10 μM haemin chloride for 24 h. *Hc-18s RNA* is used as an internal control and the $2^{-\Delta\Delta CT}$ method is used for relative transcriptional data normalisation. **j** Detection of haemozoin (absorbance at 400 nm) in the RNAi(*Hc-mrp-3*)-treated larvae after being exposed to 10, 100, and 1000 μM haemin chloride for 24 h. **k** The absorbance of haemozoin in the RNAi(*Hc-mrp-3*)-treated larvae after exposing to 100 μM haemin chloride for 24, 48 and 72 h. Data are shown as mean ± standard deviation (SD). Student's *t* test is performed for statistical analyses. **P* < 0.01, ***P* < 0.05, ****P*< 0.001. **l** A schematic diagram demonstrating the involvement of *Hc-mrp-3* in haem homeostasis under low and high concentrations of exogenous haem. In the condition of insufficient exogenous haem, *hrg-1* is upregulated while *mrp-3* is downregulated to facilitate efficient haem acquisition and utilisation; by contrast, in the condition of excessive exogenous haem, *hrg-1*, *hrg-2* and *gst-1* are downregulated, *mrp-3* is upregulated, and the formation of haemozoin is increased for efficient haem efflux and detoxification

suggests a role of *mrp-3* in dealing with extra, toxic free haem at the blood-feeding stages of this parasite (Fig. 5l).

mrp-3 gene is required for haem detoxification in the blood-feeding larvae in vitro

Using a well-established culturing system [38], we obtained L4s of *H. contortus* which usually feed on blood within host animals, by activating and culturing the infective larvae (L3s) in vitro for 4 days. In the in vitro cultured L4s, gene silencing of *Hc-mrp-3* was conducted by soaking the activated L3s with liposome-encapsulated small interfering RNAs for at least 4 days (Fig. 6a). Compared with wildtype control, RNAi(*Hc-mrp-3*) did not affect the larval development or mortality of treated larvae (Fig. 6b and c), but stimulated the survival of L2s (0.001–0.1 μM) as well as the development (0.1–1 μM) and survival (0.1 μM) of in vitro cultured L4s when supplemented with a low-concentration of haemin chloride (Fig. 6d, e and g). However, higher concentrations of exogenous haem resulted in decreased larval development (after 4 days of treatment with 10 or 100 μM haem) and survival rate (after 6 days of treatment with 100 μM haem) of RNAi(*Hc-mrp-3*)-treated larvae (Fig. 6d, f and h), suggesting a toxic nature of excessive free haem and a requirement of *Hc-mrp-3* for haem efflux and detoxification in the L4s of *H. contortus*.

Supplementing a toxic haem analogue (gallium protoporphyrin IX, GaPP IX) into the culture medium for 24 h resulted in increased larval mortality of L2s (Fig. 6i) and in vitro cultured L4s (after 72 h; Fig. 6j). The concentration of GaPP IX that killed 50% of wildtype L2s in vitro (LC_{50}) was measured at 12.00 μM. Gene silencing of *Hc-mrp-3* significantly increased the sensitivity of treated L4s to the toxic GaPP IX, with the LC_{50} measured at

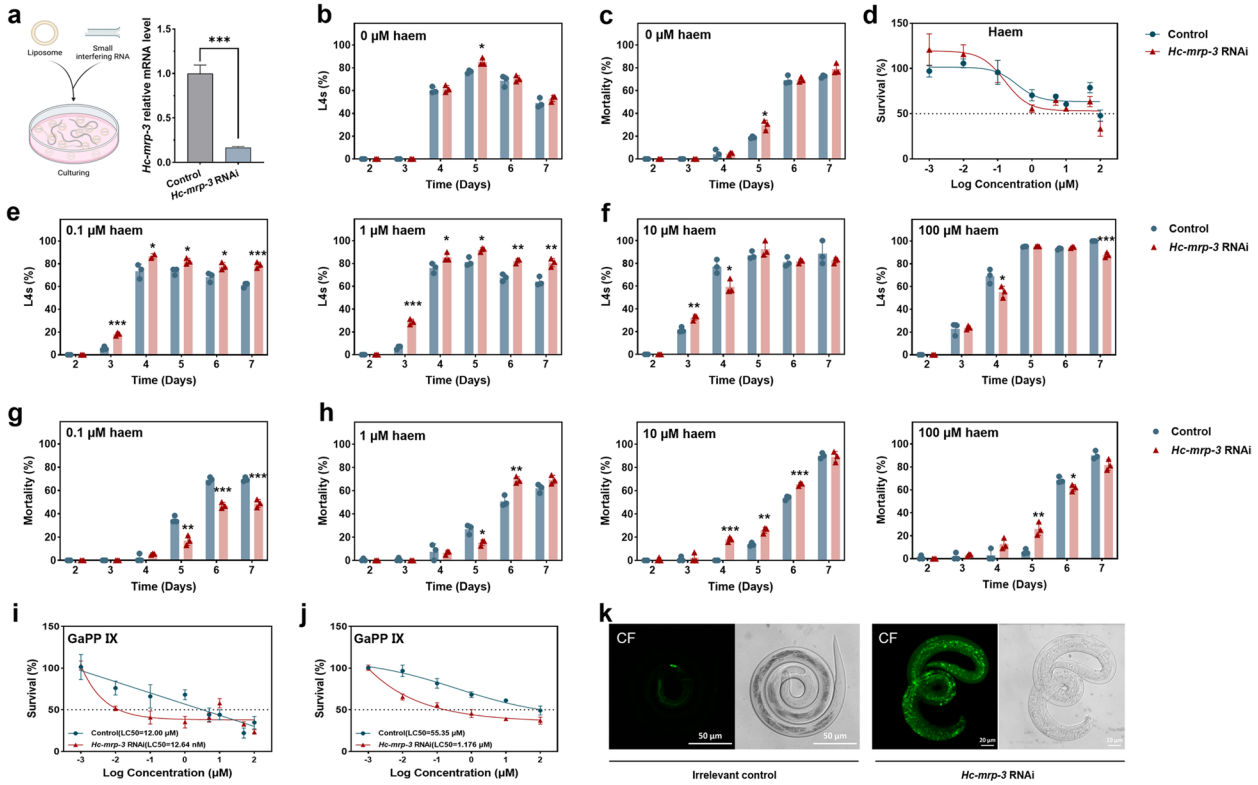

Fig. 6 RNA interference-mediated gene knockdown of *Hc-mrp-3* results in developmental deficit and lethality of *Haemonchus contortus*. **a** RNA interference of *Hc-mrp-3* using a soaking method and gene knockdown analysis in treated xL3s of *H. contortus* after 24 h. Small interfering RNA targeting *cry1Ac* of *Bacillus thuringiensis* is used as an irrelevant control. *Hc-18s RNA* is used as an internal control and the $2^{-\Delta\Delta CT}$ method is used for relative transcriptional data normalisation. Data are shown as mean ± standard deviation (SD). **b,c** Larval development and mortality of RNAi(*Hc-mrp-3*)-treated xL3s and controls during a 7-day in vitro culturing. **d** The influence of serially diluted exogenous haem (10^{-3} to 10^{2} μM) on the survival of RNAi(*Hc-mrp-3*)-treated free-living larvae (feeding method) after 24 h. **e,f** Larval development of RNAi(*Hc-mrp-3*)-treated xL3s, after being exposed to 0.1, 1, 10 and 100 μM of haemin chloride for six days. **g,h** Mortality of RNAi(*Hc-mrp-3*)-treated xL3s, after exposing to 0.1, 1, 10 and 100 μM of haemin chloride for 6 days. **i** The influence of the serially diluted (10^{-3} to 10^{2} μM) Ga (III) complex of the haem precursor protoporphyrin IX (GaPP IX; a toxic haem analogue) on the survival of RNAi(*Hc-mrp-3*)-treated larvae (feeding method) after 24 h. **j** The influence of serially diluted (10^{-3} to 10^{2} μM) GaPP IX on the survival of RNAi(*Hc-mrp-3*)-treated xL3s (soaking method) after 72 h. The mortality of larvae fed with bacteria expressing double-stranded RNA or soaked with siRNAs targeting *cry1Ac* of *Bacillus thuringiensis* (an irrelevant control) is used for data normalisation. Data are shown as mean ± standard error of the mean (SEM). Student's *t* test is performed for statistical analyses. *$P < 0.05$, **$P < 0.01$, ***$P < 0.001$. **k** The accumulation of carboxyfluorescein in RNAi(*Hc-mrp-3*)-treated xL3s, compared with untreated worms (Control). Scale bars, 20 or 50 μm

12.64 nM (Fig. 6i). The LC_{50} of GaPP IX for in vitro cultured wildtype L4s and RNAi(*Hc-mrp-3*)-treated L4s was measured at 55.35 and 1.18 μM (Fig. 6j), verifying the detoxification role of MRP-3 in *H. contortus*. The efflux role of *Hc*-MRP-3 was verified in the in vitro-cultured L4s (Fig. 6k).

Gene transcription of *mrp-3* in blood-feeding larvae is activated but not uniquely regulated by NHR-14

Given the fact that no haem-responsive element (HERE) [39] was identified for *mrp-3* in *H. contortus* and related species (Fig. S3d), we attempted to elucidate the mechanisms underlying its haem-responsive feature and its connected regulatory network of genes in haem homeostasis and detoxification.

By screening genes that are haem-responsive in the L4s of *H. contortus*, a total of 184 genes (including 106 upregulated and 78 downregulated genes) were found differentially transcribed in response to 1000 μM of haem chloride in vitro (Fig. 7a), and 645 genes (including 395 upregulated and 250 downregulated genes) in response to 10% sterile defibrinated host blood in vitro (Fig. 7b). Apart from immune-associated molecules, these upregulated genes were functionally linked to a range of pathways, including ABC transporters and lysosomes both of which are closely related to haem transport, as well as steroid hormone biosynthesis,

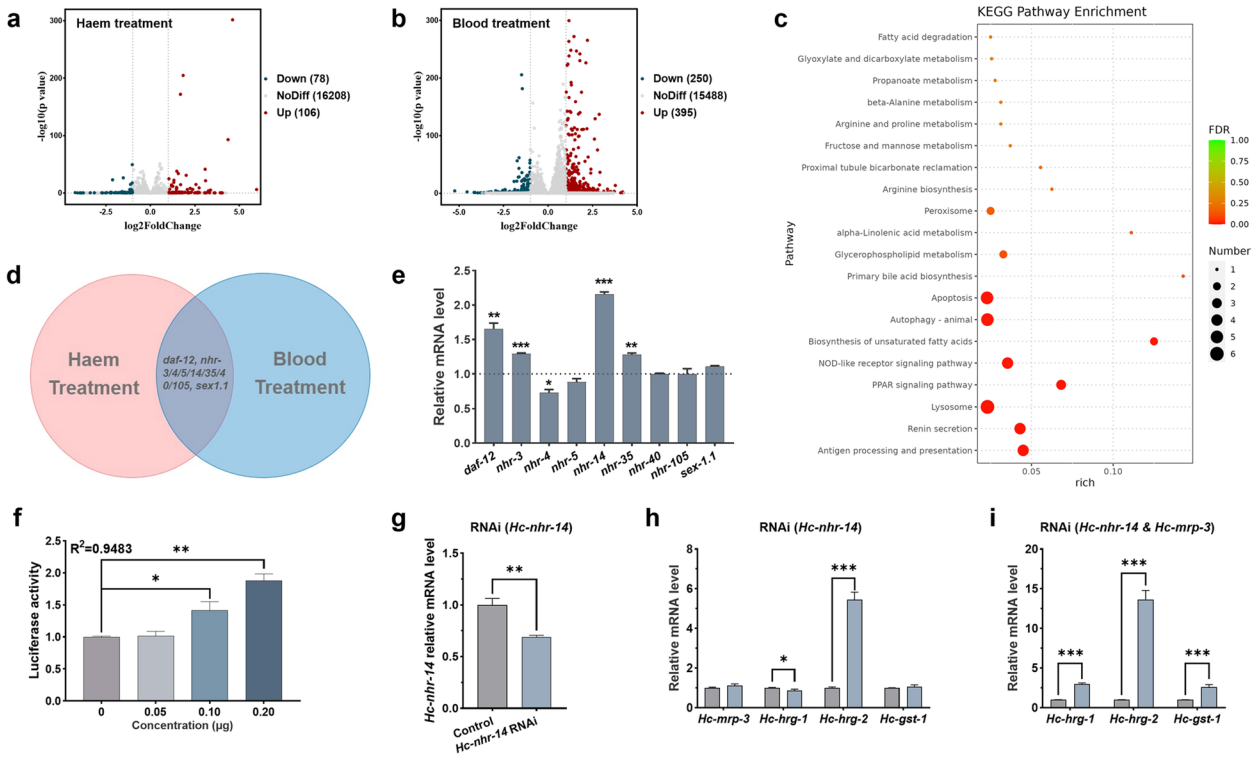

Fig. 7 Screening of haem-responsive regulator of *Hc-mrp-3* in *Haemonchus contortus*. **a,b** Comparative transcriptomic analysis of L4s and L4s of *H. contortus* exposed to 1000 μM haem or 10% sheep blood for 24 h in vitro. Treatment-induced upregulation and downregulation of genes are indicated in red and blue, respectively. **c** Enriched KEGG pathways of genes differentially expressed in haem-treated larvae of *H. contortus*. **d** Intersection of nuclear hormone receptor-coding genes(*nhr*) that are significantly changed in response to haem and blood treatment in vitro. **e** Transcriptional levels of *daf-12* and *nhr-3*, *-4*,*-5*, *-14*, *-35*, *-40*, *-105*, and *sex-1.1* in RNAi(*Hc-mrp-3*)-treated infective larvae. **f** Activation of *Hc-mrp-3* by *Hc*-NHR-14 in a luciferase reporter assay. **g** RNAi of *Hc-nhr-14*in xL3s of *H. contortus*. **h** Relative mRNA levels of *Hc-mrp-3*, *Hc-hrg-1*, *Hc-hrg-2* and *Hc-gst-1*after RNAi(*Hc-nhr-14*) treatment in xL3s of *H. contortus* for 24 h. **i** Relative mRNA levels of *Hc-hrg-1*, *Hc-hrg-2*, and *Hc-gst-1* after RNAi(*Hc-nhr-14* and *Hc-mrp-3*) treatment in xL3s of *H. contortus* for 24 h. The*cry1Ac* of*Bacillus thuringiensis* (an irrelevant control) is used as an irrelevant control. *Hc-18s RNA* is used as an internal control. A $2^{-\Delta\Delta CT}$ method is used for relative transcriptional data normalisation. Data are shown as mean± standard deviation (SD). Student's *t* test is performed for statistical analyses. **P* < 0.05, ***P*< 0.01, ****P* < 0.001

which produces ligands for nuclear hormone receptors (NHRs, a class of transcription factors) (Fig. 7c). This information suggests that NHRs might play a role in regulating the transcription of *mrp-3* in *H. contortus* during the blood-feeding stages.

Indeed, at least nine *nhr* genes were found to be upregulated or downregulated significantly in *H. contortus* in response to haemin chloride or blood treatment (Fig. 7d and Additional file 3: Table S2). Specifically, in RNAi(*Hc-mrp-3*)-treated infective larvae of *H. contortus*, mRNA levels of four *nhr* genes were significantly ($P<0.01$) increased, with *nhr-14* showing the most marked transcriptional upregulation (Fig. 7e), suggesting a role of NHR-14 (essentially a transcription factor) in regulating the transcription of *Hc-mrp-3* in *H. contortus*. Using a luciferase assay, we verified that *Hc*-NHR-14 activated the transcription of *Hc-mrp-3* in transfected HEK 293 T cells, in a dose-dependent manner ($R^2=0.9483$; Fig. 7f). Furthermore, with reference to control, gene knockdown of *Hc-nhr-14* (Fig. 7g) induced higher mRNA levels of *Hc-hrg-2* ($P<0.001$) and *Hc-gst-1*, while a lower mRNA level of *Hc-hrg-1* was found in the treated larvae of *H. contortus* (Fig. 7h). Gene knockdown of *Hc-nhr-14* did not significantly influence the transcription of *Hc-mrp-3* ($P>0.05$) (Fig. 7h). Simultaneous gene knockdown of *Hc-mrp-3* and *Hc-nhr-14* resulted in higher mRNA levels of *Hc-hrg-1* ($P<0.001$), *Hc-hrg-2* ($P<0.001$), and *Hc-gst-1* ($P<0.001$) (Fig. 7i). These results suggest that NHR-14 is unequivocally a regulator (but may not be the unique and principal one) of *Hc-mrp-3* gene transcription and is very likely involved in haem homeostasis in *H. contortus*.

mrp-3 and *nhr-14* are essential for the blood-feeding larvae to cope with extra haem

In RNAi(*Hc-mrp-3*)-treated L4s of *H. contortus*, 10 μM of haemin chloride (which resulted in increased haemozoin and larval mortality; cf. Figures 5j and 6d) was linked to an upregulation of *Hc-nhr-14* (Fig. 8a); in

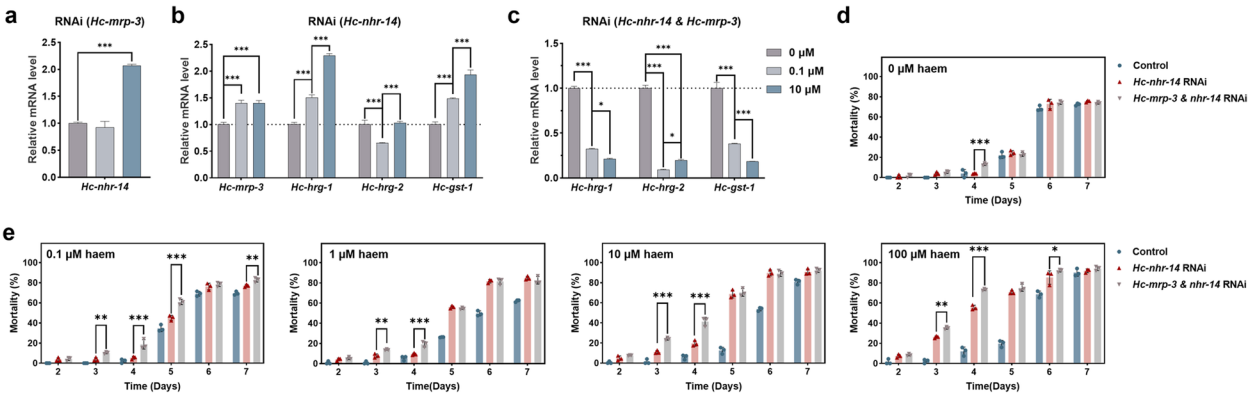

Fig. 8 The involvement of *Hc-nhr-14* and *Hc-mrp-3* in the haem detoxication of *Haemonchus contortus*. **a** Relative mRNA level of *nhr-14* in RNAi(*Hc-mrp-3*)-treated exsheathed L3s (xL3s) after exposure to 0.1 and 10 μM haemin chloride for 1 h.**b** Relative mRNA levels of *Hc-mrp-3*, *Hc-hrg-1*, *Hc-hrg-2* and*Hc-gst-1* in RNAi(*Hc-nhr-14*)-treated xL3s of *H. contortus*, after being exposed to 0.1 and 10 μM haemin chloride for 24 h. **c** Relative mRNA levels of *Hc-hrg-1*, *Hc-hrg-2* and *Hc-gst-1* in RNAi(*Hc-nhr-14* and *Hc-mrp-3*)-treated xL3s of *H. contortus*, after being exposed to 0.1 and 10 μM haem chloride for 24 h. *Hc-18s RNA* is used as an internal control. A $2^{-\Delta\Delta CT}$method is used for relative transcriptional data normalisation. Data are shown as mean ± standard deviation (SD). Student's *t* test is performed for statistical analyses. **d** Mortality of RNAi(*Hc-nhr-14*)-, RNAi(*Hc-nhr-14* and *Hc-mrp-3*)-treated xL3s and irrelevant control during a 7-day in vitro culturing. **e** Mortality of RNAi(*Hc-nhr-14*)-, RNAi(*Hc-nhr-14* and *Hc-mrp-3*)-treated xL3s and irrelevant control when exposed to 0.1, 1, 10 and 100 μM of haemin chloride for 6 days. Data are shown as mean ± standard error of the mean (SEM). Two-way ANOVA is performed for statistical analyses. **P* < 0.05, ***P*< 0.01, ****P* < 0.001

RNAi(*Hc-nhr-14*)-treated L4s, either 0.1 or 10 μM of haemin chloride significantly ($P<0.001$) increased the mRNA levels of *Hc-mrp-3*, *Hc-hrg-1* and *Hc-gst-1* (Fig. 8b); in RNAi(*Hc-mrp-3* and *Hc-nhr-14*), both 0.1 and 10 μM of haemin chloride significantly ($P<0.001$) decreased the mRNA levels of *Hc-hrg-1*, *Hc-hrg-2* and *Hc-gst-1* (Fig. 8c), compared with the larvae that were not exposed to exogenous haem. The transcriptional relationships among genes *Hc-nhr-14* and *Hc-hrg-1*, *Hc-hrg-2*, *Hc-gst-1* indicate the role of *Hc-nhr-14* in haem homeostasis.

Although RNAi(*Hc-nhr-14*) did not affect the survival of in vitro cultured L4s of *H. contortus* (Fig. 8d), it increased the mortality of treated larvae when exposed to 0.1–100 μM exogenous haem (Fig. 8e). The sensitivity of RNAi(*Hc-nhr-14*)-treated larvae to exogenous haem was even enhanced by simultaneously knocking down *Hc-mrp-3* in *H. contortus* (Fig. 8e and Additional file 2: Fig. S3c). These results show that both *Hc-mrp-3* and *Hc-nhr-14* are required for haem homeostasis and detoxification in *H. contortus* L4s, representing target candidates against the blood-feeding stages of this parasite within host animals.

Discussion

Nematode parasites usually lose metabolic complexity and rely on the host environment for nutrient provision, causing immense harm to infected humans and animals [40]. Understanding the fundamental biology of these pathogens within host animals is efficient in screening the "Achilles heel" for the development of novel intervention targets, since there is a lack of vaccines for most parasitic worms. For instance, parasitic nematodes cannot synthesise haem de novo and must acquire this essential nutrient from the environment or the host animals [15, 16], thus the chokepoint of haem acquisition (i.e. only one haem importer has been found in a wide range of parasitic nematodes) represents an intervention target for the control of nematode infection [27, 30]. However, compared with the "bright side" of haem in nematodes [15], little is known about how nematodes survive from the cytotoxicity of this molecule (the "dark side"), particularly for haemophagous species in which red blood cells are ruptured and release a large amount of free haem. In the current work, we report a novel efflux machinery for haem detoxification in a blood-feeding nematode.

The first key component of the haem efflux machinery is MRP-3, a specific member of the multidrug resistance protein (MRP) family known for their ABC transporter activity and roles in anthelmintic resistance [41–44]. Although *mrp-5* gene has been reported to play a role in haem trafficking from the intestine to the pseudocoelom in the free-living nematode *C. elegans* [19] and haem-responsive in *Brugia malayi*, a causative agent of lymphatic filariasis [30], *mrp-3* gene appears to be more sensitive to exogenous haem in the *H. contortus*, and thus likely more important for this and related blood-feeding nematodes. After systematic explorations, we demonstrate that MRP-3 protein is dominant in the inner membrane of hypodermis (which usually adheres to the excretory column) and the intestine of adult *H. contortus*, functions in haem analogue efflux, is involved in a

gene network for haem homeostasis, and is required for haem detoxification. In addition, stronger evidence is that there is an increased level of haem pigment (known as haemozoin, usually found in haem detoxification processes) [7] in the RNAi(*mrp-3*)-treated larvae of *H. contortus*, particularly in response to haem exposure. Clearly, *mrp-3* encodes an exporter of substrates and is required for haem detoxification in blood-feeding nematodes. Surprisingly, although the *mrp-3* gene exhibits a haem responsive feature and is tightly regulated for haem homeostasis, the canonical responsive element (i.e. HERE) [39] for haem responsive genes is not predicted in *H. contortus* and other related nematodes. A better understanding of this mystery should provide more biological details for MRP-3 in haem efflux and detoxification.

Indeed, the nuclear hormone receptor NHR-14 is elucidated to activate the transcription of *mrp-3*, representing a possible regulatory component of the haem efflux machinery in *H. contortus*. NHR-14 is a member of the protein superfamily characterised by a modular architecture of DNA-binding domain and ligand-binding domain in multicellular organisms [45, 46], usually functions as ligand-activated transcription factors in regulating gene transcription in metazoans [47]. The most famous nuclear hormone receptor in nematodes is DAF-12, which controls the exit from the dauer stage of *C. elegans* and the activation of infective larvae of parasitic nematodes via regulating an intricate network of genes and microRNAs [48–52]. In this work, using a transcriptomic screening approach, we identified that NHR-14 is related to the haem exposure and the regulation of *mrp-3*, and tested that this protein is indeed involved in haem homeostasis and required for haem detoxification in *H. contortus*. Although NHR-14 has been reported to play roles in DNA-damage-induced apoptosis and intestinal iron uptake in *C. elegans* [53, 54], little is known about its role in the haem detoxification of blood-feeding nematodes. Nonetheless, gene silencing of *nhr-14*, though not sufficient, is linked to an increased sensitivity of treated worms to exogenous haem; simultaneous gene knockdown of both *mrp-3* and *nhr-14* can result in a higher lethality of treated worms, verifying the crucial role of NHR-14 in haem detoxification. However, *nhr-14* RNAi did not significantly influence the transcription of *mrp-3*. The haem regulation of *mrp-3* is likely a non-specific, haemostasis-associated secondary effect, which can be explained by the biological fact that MRP-3 is not a haem-specific transporter. Apart from *nhr-14*, the role of other *nhr* genes affected by *mrp-3* RNAi also warrants further investigations.

Molecules previously known to be involved in nematode haem homeostasis are also major components of the haem efflux machinery in blood-feeding nematodes. In *H. contortus*, we found that there is a clear relationship between the genes involved in haem acquisition (e.g. *hrg-1*), haem binding (e.g. *hrg-2* and *gst-1*) and haem export (e.g. *mrp-3*): when there is sufficient haem in worms, haem acquisition will be decreased while haem transport and export increased; perturbation of *mrp-3* (and *nhr-14* although not fully elucidated) involved in haem efflux results in an accumulation of haem and death of worms. Although there are some genetic and functional discrepancies between free-living and parasitic nematodes, these molecules are well conserved in a wide range of parasitic nematodes of humans and animals. Nuclear hormone receptors and ABC transporters have already been proposed as potential intervention targets for parasitic nematodes [55]. Our findings indicate that NHR-14 and MRP-3 are the most promising target candidates for *H. contortus* and related parasites. Further investigations of endogenous and exogenous ligands that activate NHR-14 and whether the ligand-activated receptor regulates the transcription of other haem-responsive genes should provide more implications for the biological research of blood-feeding nematodes.

Conclusions

In conclusion, we demonstrate that MRP-3 plays a role in haem efflux and is required for haem detoxification in a haematophagous nematode. The role of MRP-3 in haem efflux is somehow associated with the nuclear hormone receptor NHR-14, and gene silencing of MRP-3 and NHR-14-coding genes markedly compromised the survival of worms exposed to exogenous haem. These findings provide novel insights into the haem biology of parasitic worms and indicate potential targets for the intervention of parasitic diseases in humans and animals.

Methods

Cell line, yeast mutant and nematode

The human embryonic kidney (HEK) 293 T cell line was purchased from IMMOCELL (Kunming, China) and maintained according to the manufacturer's instructions. The *Δhem1* mutant of yeast (*Saccharomyces cerevisiae*) was constructed as described in our recent work [27] and maintained in a 2% glucose synthetic complete (SC; -LEU) medium supplemented with 250 μM 5-aminolevulinic acid (ALA; Sigma-Aldrich, USA) at 30 °C. The eggs, first- (L1s), second- (L2s), third- (L3s), exsheathed L3s (xL3s), and fourth-stage larvae (L4s; in vitro and in vivo), and adults of *H. contortus* (ZJ strain) were produced using well-established protocols as described previously [27, 56].

Genome-wide identification

Genes coding for MRPs in *H. contortus* and other parasitic nematodes were predicted using the EnsemblCompara GeneTrees pipeline [57], with reference to the *mrp* genes of *C. elegans*, the free-living model organism. Nucleotide acid sequences of *mrp* gene candidates and deduced amino acid sequences were obtained from the WormBase ParaSite database (version: WBPS17) (https://parasite.wormbase.org/). To confirm sequence integrity, a domain architecture analysis was performed for the deduced amino acid sequences using InterProScan v.5.24.63 [58]. Full-length sequences were aligned, and the likelihood of these sequences was calculated on a maximum-parsimony guide tree for all relative homologues using MEGA X v.10.1.8 [59].

Transcriptional profiling

RNA-seq data sets (SRP928055, SRP928056, SRP928057, SRP928058, SRP928059, SRP928060, SRP928061, SRP928062, SRP928063, SRP136037) publicly available for *H. contortus* (Haecon-5 strain) were downloaded from the sequence read archive (SRA) at the National Center for Biotechnology Information [56, 60]. Clean reads were mapped to the reference genome of *H. contortus* (BioProject PRJEB506; haemonchus_contortus_MHCO3ISE_4.0; [61]) using Bowtie v.2.1.0 within the software package RSEM v.1.2.11 [62, 63]. The count of reads that were mapped to gene models (including curated *mrp* genes) was normalised as transcripts per million (TPM) among the key developmental stages (i.e. egg, L1, L2, L3, L4, and adult) of *H. contortus* or experimental conditions (e.g. L3s, xL3s, and L4s), then visualised in heatmaps using pheatmap v.1.0.12.

Haem response assay

The larvae (L2s) of *H. contortus* were washed in antibiotic–antimycotic solution (10 μg/ml amphotericin B, 100 U/ml streptomycin, 100 U/ml penicillin, 40 μg/ml gentamycin and 100 μg/ml ampicillin) at room temperature. The adults (females and males mixed) of *H. contortus* were extensively washed in a prewarmed (37 °C) antibiotic–antimycotic solution. Sterilised worms were then transferred to RPMI 1640 medium (25 mM HEPES, 5 mM glutamine, 1% FBS, 100 U/ml streptomycin, 100 U/ml penicillin, and 2 μg/ml amphotericin B) supplemented with 0, 10 or 100 μM haemin chloride (Sigma-Aldrich, USA) and incubated at 28 °C or 10% CO_2, 37 °C for 24 h. After incubation, the worms were harvested by centrifugation (1000 × *g* for larvae collection while flash for adult collection) for 5 min, washed three times in PBS, snap frozen in liquid nitrogen and stored at − 80 °C until use. The mRNA levels of *Hc-mrp-3* in the larvae and adults in response to haemin chloride exposure (0, 10 and 100 μM) were determined using quantitative real-time polymerase chain reaction (qRT-PCR) assays.

qRT-PCR

Total RNAs were extracted from each sample of the eggs, larvae and adults, or treated or untreated larvae of *H. contortus* using the TRIzol reagent (Invitrogen, USA), following the manufacturer's protocols. Complementary DNA (cDNA) was synthesised using a ReverTra Ace qPCR RT Kit (Toyobo, Japan); then diluted cDNA was used to amplify the sequence of *mrp-1/2*, *mrp-3*, *mrp-4*, *mrp-5*, *mrp-6*, *mrp-7*, and related genes (e.g. *Hc-hrg-1*, *Hc-hrg-2*, *Hc-gst-1* and related *nhr* genes) employing an SYBR Green real-time PCR master kit (Toyobo, Japan), according to the manufacturer's instructions, on a LightCycle 480 system (Roche, Basel, Switzerland). At least three biological or technical replicates of each sample were assessed, with the small subunit of the nuclear ribosomal RNA gene (*18S RNA*) used as an internal control [64]. A $2^{-\Delta\Delta CT}$ method was used to analyse the transcriptional changes of a specific gene [65]. The primer sets used in this experiment are shown in Additional File 4: Table S3. At least three technical replicates were included for the data collection and analysis.

Lentivirus transduction

The coding sequence of *Hc-mrp-3* was cloned into the pLenti CMV GFP Puro vector (pLenti CMV GFP Puro (658–5) was a gift from Eric Campeau & Paul Kaufman (Addgene plasmid # 17,448; http://n2t.net/addgene:17448; RRID: Addgene_17448) [66] via the *Xbal* I and *Sal* I sites. The recombinant pLenti CMV GFP Puro-*Hc-mrp-3*-Flag plasmids were introduced into HEK 293 T cells with psPAX2 and pMD2.G after packing with lipofectamine 2000 (Invitrogen, USA). Infectious lentivirus particles were harvested from the DMEM culture medium after 48 h by centrifugation at 800 × *g* at 4 °C for 5 min, then filtered through a 0.45-μM-pore cellulose acetate filter. The purified lentivirus particles (1.5 mL) were added to the culture medium to transduce HEK 293 T cells in 6-well plates at 37 °C, 5% CO_2 for 24 h. The transduced cells were treated with 0.5 μg/mL puromycin for 3 generations and then screened for monoclonal cells to obtain resistant or positive colonies.

Subcellular localisation

The subcellular localisation was conducted using a well-established method [27]. In brief, the coding sequence of *Hc-mrp-3* was cloned into the pLenti CMV GFP/FLAG Puro vector via the *BamH I* and *Xba I* site. The recombinant plasmid was transiently transfected or co-transfected with hRab5a or hRab7a recombinant plasmids into HEK 293 T or Hela cells in laser confocal Petri

dishes using lipofectamine 2000 (Invitrogen, USA). The transfected cells were stained in Lyso-Tracker Red (Beyotime, China) or DiI staining kit (Beyotime, China) using the manufacturer's protocols. Cell nuclei were stained using DAPI (Beyotime, China). Subcellular localisation was determined by confocal microscope (LSM880, Carl Zeiss).

Flow cytometry

The fluorescence efflux assay was conducted using a well-established method [20, 34, 67]. In brief, 2 μM of Calcein-AM (Beyotime, China), 5 μM of 5(6)-carboxyfluorescein (Sigma-Aldrich, USA) or 20 μM of ZnMP (Frontier Scientific, USA) were added into the culture medium DMEM of resuspended HEK 293 T cells at 37 °C, 5% CO_2 for 30 min or 2 h (ZnMP); then, the cells were washed with PBS and resuspended in fresh DMEM and incubated at 37 ℃, 5% CO_2 for 30 min. After washing in PBS, fluorescence-activated cell sorting analysis was performed on a flow cytometer (BD Bioscience, USA). Rhodamine 123 (2.5 μM) (Beyotime, China) was used as a control [67]. An inhibitor for MRP-1 known as MK571 (10 μM) [33] was used to inhibit the function of *Hc*-MRP-3. The data were calculated as the ratios of the mean fluorescence intensity of wild-type HEK293T cells for the efflux assay.

Heterologous expression

The coding sequence of *Ce-hrg-4* or *Hc-mrp-3* was inserted into the pYES2/CT vector (Thermo Fisher, USA) via the *Hind* III and *Kpn* I sites. After sequencing, the recombinant plasmids were transformed into the *Δhem1* yeast cells using a lithium acetate method [68, 69]. Transformed yeast was inoculated on a 2% glucose synthetic complete (SC; -Ura/-LEU) plate supplemented with 250 μM ALA, then streaked onto a 2% raffinose SC (-Ura/-LEU) plate supplemented with 250 μM ALA. Transformants were inoculated into a 2% raffinose SC (-Ura/-LEU) liquid medium supplement with 0.4% galactose and 250 μM ALA, collected at mid-log phase, and fixed with 3.7% paraformaldehyde (PFA) for 1 h at room temperature.

Yeast spotting and growth assays

A colony of transformed yeast was inoculated into a 2% raffinose SC (-Ura/-LEU) medium and cultured for 18 h to deplete haem, then diluted in water (OD600 = 0.2). tenfold-serial dilution (5 μL) of transformant was spotted onto a 2% raffinose SC (-Ura/-LEU) plate supplemented with haemin chloride (0.5, 1 or 2.5 μM), 250 μM ALA (positive control) or water (negative control), and 0.4% galactose, incubated at 30 °C for 3 days, and imaged. Growth curves of *Δhem1* were determined by measuring the OD600 after culturing cells (OD600 = 0.1) in 2% raffinose SC (-Ura/-LEU) liquid medium supplemented with 2.5 μM haem or 250 μM ALA and 0.4% galactose after 14, 16, 18, 20, 22 and 24 h.

Immunofluorescence assay

The HEK 293 T cells were cultured to 80–90% confluent in laser confocal a petri dish and fixed with cold methanol at − 20 ℃ for 15 min. The fixed cells were blocked with 0.1% BSA at 37 ℃ for 1 h, incubated with primary antibodies (rabbit anti-Flag; Cell Signaling Technology, USA) at a 1:1000 dilution at 37 ℃ for 1 h, then with a goat anti-rabbit IgG(H + L) Cross-Adsorbed ReadyProbe Secondary Antibody, Alexa Fluo 488 (Invitrogen, USA) at a 1:1000 dilution at 37 ℃ for 1 h. The nuclei were stained with 0.5 μg/mL 4',6-diamidino-2-phenylindole (DAPI) (Sigma-Aldrich, USA) at room temperature for 30 min.

Immunofluorescence assay on yeast cells was performed using a well-established method [68]. In brief, yeast cells were cultured to mid-log phase and fixed with 3.7% w/v formaldehyde for 1 h at room temperature; the fixed cells were washed with 100 mM potassium phosphate buffer, pH 6.5, then digested with sorbitol phosphate-citrate buffer (SPC) containing 10% glusulase and 0.01% zymolyase 20 T for 90 min at 30 °C; the digested cells were washed and added onto poly-L-lysine-coated slides at room temperature for 5 min then with cold methanol for 5 min, and blocked with PBS containing 2% milk and 0.1% Tween-20 at room temperature for 5 min. The blocked cells were incubated with the primary antibodies (rabbit anti-Flag; Cell Signaling Technology, USA) at a 1:1000 dilution at 37 ℃ for 1 h, then with a goat anti-rabbit IgG(H + L) Cross-Adsorbed ReadyProbe Secondary Antibody, Alexa Fluo 488 (Invitrogen, USA) at a 1:1000 dilution at 37 ℃ for 1 h.

For the immunofluorescence assay on *H. contortus*, adult worms (females and males) were fixed in 4% paraformaldehyde for 48 h, embedded in paraffin and processed for 5-μm tissue sections. Worm sections were bathed in 100 °C citrate antigen retrieval solution (pH 6.0) for 20 min, blocked in 10% donkey serum (Absin, Shanghai, China) at 4 °C overnight. Blocked sections were incubated with a primary antibody (mouse anti-*Hc*-MRP-3 polyclonal antibodies, prepared internally) at a 1:200 dilution, followed by a donkey anti-mouse IgG (H + L) ReadyProbe Secondary Antibody, Alexa Fluo 488 (Invitrogen, USA) at a 1:1000 dilution, then stained with 0.5 μg/mL 4',6-diamidino-2-phenylindole (DAPI) (Sigma-Aldrich, USA) for 30 min. Images were taken using an LSM880 confocal microscope (Zeiss, Germany).

dsRNA-mediated RNAi in L2s

A feeding method was used to conduct gene silencing of *Hc-mrp*-3 in the free-living stages of *H. contortus* as described previously [27, 70]. In brief, a fragment of *Hc-mrp-3* coding sequence was cloned and inserted into the L4440 vector via the *Hind* III and *Kpn* I sites. *Escherichia coli* HT115 transformed with the recombinant plasmids was used to feed the newly hatched larvae of *H. contortus*. The larvae were incubated at 28 °C with 80% relative humidity for 6–10 days. The phenotypes of treated larvae were monitored in aspects of development, motility, and death every day. *Bt-cry1Ac* from *Bacillus thuringiensis* (GenBank accession no. GU322939.1) was used as an irrelevant control [71]. The mRNA levels of *Hc-mrp-3* in treated and untreated larvae were determined using qRT-PCR and analysed using the $2^{-\Delta\Delta CT}$ method. Primer sets are shown in Additional File 4: Table S3.

Nematode fluorescence efflux assay

A fluorescence efflux assay was performed on the early stages of *H. contortus* using a method modified from a previous work [72]. In brief, about 1000 RNAi(*Hc-mrp-3*)-treated L2s were collected, washed thoroughly in sterile water and centrifuged at 1000×*g* for 5 min. Purified larvae were incubated with 4 μM of calcein-AM, 4 μM of 5(6)-CFDA, 1.5 μM of Rho123, or 50 μM of ZnMP in sterile water at 28 ℃ with shaking for 60 min (for calcein-AM and 5(6)-CFDA), or 15 min (Rho123) or 4 h (ZnMP), respectively, then washed three times; the larvae were resuspended in sterile water at 28 ℃ with shaking for 30 min (for calcein-AM and 5(6)-CFDA), 15 min (Rho123) or 1 h (ZnMP), respectively. After centrifugation at 1000×*g* for 5 min, the larvae were examined under an LSM880 confocal microscope (Zeiss, Germany), whereas the supernatant was analysed using a Synergy H1 microplate reader (Biotek, USA). Untreated larvae were used as a control.

siRNA-mediated RNAi in L4s

Small interfering RNA (siRNA) was used to knock down *Hc-mrp*-3 in the L4 stage of *H. contortus* in vitro, using a soaking method modified from previous publications [73, 74]. Briefly, specific siRNAs targeting the coding sequence of *Hc-mrp*-3 were designed using an online server DSIR (http://biodev.extra.cea.fr/DSIR/DSIR.html), then synthesised and packed with a Lipofectamine RNAiMAX reagent (Thermo Fisher, USA). The infective larvae were exsheathed in 0.15% hypochlorite with shaking at 37 °C for 20 min, washed three times in sterile physiological saline, transferred to prewarmed DMEM (~6000 larvae per mL) containing 1% Antibiotic–Antimycotic (Fdbio Science, China), and cultured at 38 ℃, 10% CO_2 for 96 h. The packed siRNAs (2 pmol) were added into the culture medium and incubated at 38 °C, 10% CO_2 for 48 h. siRNA from *Bt-cry1Ac* was used as an irrelevant control. The mRNA levels of *Hc-mrp-3* in treated and untreated larvae were determined using qRT-PCR and analysed using the $2^{-\Delta\Delta CT}$ method. Primer sets are shown in Additional File 4: Table S3.

Haemozoin analysis

The isolation and quantification of haemozoin in *H. contortus* were performed as described previously [29, 75]. In brief, about 600 *H. contortus* L4s were treated with siRNAs targeting *Hc-mrp-3* or *Bt-cry1Ac* and exposed to 0, 10, 100 and 1000 μM haemin chloride for 24 h in vitro. Treated worms were washed three times with sterile physiological saline, then homogenised and centrifuged at 1500 *g* for 30 s. The consequent supernatant was centrifuged at 12,000 *g* for 15 min, and the pellets were washed three times with sterile physiological saline and dissolved in a 0.1 M NaOH solution. The absorbance of the prepared sample was determined at 400 nm wavelength using a Synergy H1 microplate reader (Bio Tek, USA).

Larval development and mortality assays

The development and death rate of treated larvae of *H. contortus* in vitro were determined as described previously [27, 76]. In brief, RNAi(*Hc-mrp-3*)- or RNAi(*Bt-cry1Ac*)-treated larvae were exposed to 0, 0.1, 1, 10 or 100 μM haemin chloride in RPMI culture medium and incubated at 38 ℃, 10% CO_2. The numbers of developed L4s and dead larvae were calculated every 24 h, and the larval development rate and mortality rate were calculated with reference to the blank or irrelevant control at each time point. At least three biological replicates were included for the data collection and analysis.

RNA-seq

The in vitro cultured L4s ($n \approx 10{,}000$) of *H. contortus* were exposed to sterile physiological saline, 1000 μM of haemin chloride or 10% sterile defibrinated blood at 38 ℃, 10% CO_2 for 24 h. Total RNA was extracted from three replicates of each treatment using the TRIzol reagent (Invitrogen, USA). High-quality mRNA was isolated using magnetic beads with Oligo(dT), cleaved into short fragments about 300 bp in length, and subjected to complementary DNA synthesis and library construction. Libraries were evaluated using the Agilent 2100 Bioanalyzer (Agilent, USA), then sequenced on the Illumina Novaseq 6000 platform. After data filtration, clean reads were mapped to the reference gene models of *H. contortus* (BioProject PRJEB506) [61]. Read count normalisation, difference expression analysis, enrichment analysis and clustering analysis were performed as

described previously [56]. Fold change ≥ 2 and adjusted *P* value ≤ 0.05 were used as thresholds for differentially transcribed genes.

Luciferase reporter assay

A dual-luciferase reporter assay was performed using a well-established method [77]. In brief, 0.2 μg of pcDNA3.1-*nhr-14*, 0.1 μg pcDNA3.1-*nhr-14* and 0.1 μg vector, 0.05 μg pcDNA3.1-*nhr-14* and 0.15 μg vector, or 0.2 μg vector were co-transfected with pGL4.20-*Hc-mrp-3*-Promoter and pRL-SV40 into HEK 293 T cells in a 24-well plate. Cells were harvested at 24 h after transfection, and luciferase activity was measured using a Dual-Lumi II Luciferase Assay Kit (Beyotime, China) following the manufacturer's instructions. Luminescence was measured with a Synergy H1 microplate reader (Bio Tek, USA).

Statistical analysis

More than three biological (data presented as mean ± standard error of the mean) or technical replicates (data presented as mean ± standard deviation) were included in each assay. Statistical analysis was performed using the Student *t* test, one-way ANOVA or two-way ANOVA in GraphPad Prism 9 (San Diego, CA, USA). $P < 0.05$ was considered statistically significant unless specified.

Abbreviations

ALA	δ-Aminolevulinic acid
BSA	Bovine serum albumin
CF	Carboxyfluorescein
DAPI	4′,6-Diamidino-2-phenylindole
FPKM	Fragments per kilobase million
GaPP IX	Gallium protoporphyrin IX
MFI	Mean fluorescence intensity
Rho123	Rhodamine 123
SPC	Sorbitol phosphate-citrate buffer
TPM	Transcripts per million
ZnMP	Zinc mesoporphyrin IX

Supplementary Information

The online version contains supplementary material available at https://doi.org/10.1186/s12915-024-02001-0.

Additional file 1: Table S1. List of multiple drug resistance protein family orthologues identified in 26 parasitic nematodes of animals or humans.

Additional file 2: Fig. S1. A schematic diagram demonstrating lentivirus-mediated stable cell line construction and the fluorescence efflux assay. The diagram shows lentivirus-mediated heterologous expression of*Hc*-MRP-3 with Flag tag in the human embryonated kidney (HEK 293T) cell line and the fluorescence efflux assay. The protein expression of *Hc*-MRP-3-Flag in HEK 293T cells is confirmed by an indirect immunofluorescence assay using anti-Flag antibodies (right subpanel). Scale bar, 2 μm or 5 μm as indicated. Fig. S2. Indirect immunofluorescence assay of MRP-3 in the adults of *Haemonchus contortus*. Tissue localization (green) of MRP-3 protein in the female (a) and male (b) adults of *H. contortus* is indicated using inner-prepared polyclonal antibodies against *Hc*-MRP-3. The nuclei are stained with 4′,6-diamidino-2-phenylindole (DAPI) and indicated in blue. Scale bar, 50 μm, 20 μm or 10 μm. (c) A schematic diagram illustrates the tissue expression patterns of *Hc*-HRG-1, *Hc*-HRG-2 and *Hc*-MRP-3 (created in Biorender). The tissue expression pattern of *Hc*-MRP-3 is partially overlapped with that of *Hc*-HRG-2 in *H. contortus*. Fig. S3. Mechanism underlying the haem responsive feature for *mrp-3* in *Haemonchus contortus*. (a) Relative mRNA level of *Hc-mrp-3* in the egg, first- (L1s), second- (L2s), third- (L3s) and fourth-stage larvae (L4s), and adults of *H. contortus*. *Hc-18s RNA* is used as an internal control. One-way ANOVA is used for statistical analyses. A different letter among the data indicates a significant difference. Relative mRNA levels of *Hc-mrp-3* (b) in RNA interference (*Hc-mrp-3*)-treated L2s and *Hc-mrp-3* and *Hc-nhr-14* (c) in irrelevant and RNA interference (*Hc-mrp-3* and *Hc-nhr-14*)-treated exsheathed L3s after 24 h. *Hc-18s RNA* is used as an internal control. A $2^{-\Delta\Delta CT}$ method is used for relative transcriptional data normalisation. Data are shown as mean ± standard deviation (SD). Student t-test is performed for statistical analyses. ***$P < 0.001$. (d) Prediction of haem responsive element (HERE) for *Hc-mrp-3* and its orthologues, as well as *Hc-mrp-1/2* and *Hc-mrp-5* in blood-feeding nematodes, with information from *Caenorhabditis elegans*.

Additional file 3: Table S2. Nuclear hormone receptors that are significantly regulated in response to haem or blood.

Additional file 4: Table S3. Primer sets used in PCR for molecular cloning, heterologous expression, quantitative real-time PCR and RNA interference.

Additional file 5: Table S4. Detailed information for data values used for diagrams.

Acknowledgements

We are grateful to the technical assistance from staff in the Experimental Teaching Center, and the Shared Management Platform for Large Instrument, College of Animal Sciences, the Analysis Center of Agrobiology and Environmental Sciences, Zhejiang University. Comments from Professor Caiyong Chen from the College of Life Sciences and Innovation Center for Cell Signaling Network, Zhejiang University, China, are highly appreciated during experiments and the drafting of this manuscript.

Authors' contributions

GM supervised the whole project. AD, DT and FW conceived, designed the project. XC, DT, JRZ and JJZ contributed to the acquisition, analysis and interpretation of data. ZD contributed to the RNA-seq data analysis. DT and FW have drafted the work. Y.Y., A.D. and G.M. revised the manuscript. AD, FW and GM contributed to the funding acquisition. All authors read and approved the final manuscript.

Funding

This work is supported by the National Natural Science Foundation of China (32473050 to GM, 32172877 to AD and 32202829 to FW), and the Natural Science Foundation of Zhejiang Province (LZ22C180003 to GM).

Availability of data and materials

All data presented in diagram are included as supplementary information files. Nucleic acid sequence data are accessible via the National Center for Biotechnology Information (NCBI) sequence reads archive (SRA) under accession number PRJNA1050045. Nucleic acid sequence data sets analysed during this study are accessible via WormBase Parasite (PRJEB506 [32, 61]) or SRA (SRP026668 [60]).

Declarations

Ethics approval and consent to participate

Not applicable.

Consent for publication

Not applicable.

Competing interests

The authors declare that they have no competing interests.

Received: 27 February 2024 Accepted: 2 September 2024
Published online: 11 September 2024

References

1. Chambers IG, Willoughby MM, Hamza I, Reddi AR. One ring to bring them all and in the darkness bind them: The trafficking of heme without deliverers. Biochim Biophys Acta Mol Cell Res. 2021;1868(1):118881. pmid: 33022276.
2. Shimizu T, Lengalova A, Martínek V, Martínková M. Heme: emergent roles of heme in signal transduction, functional regulation and as catalytic centres. Chem Soc Rev. 2019;48(24):5624–57 pmid: 31748766.
3. Voltarelli VA, Alves de Souza RW, Miyauchi K, Hauser CJ, Otterbein LE. Heme: The Lord of the Iron Ring. Antioxidants (Basel). 2023;12(5):1074 pmid: 37237940.
4. Kumar S, Bandyopadhyay U. Free heme toxicity and its detoxification systems in human. Toxicol Lett. 2005;157(3):175–88 pmid: 15917143.
5. Gorman MJ. Iron homeostasis in insects. Annu Rev Entomol. 2023;68:51–67 pmid: 36170642.
6. Kořený L, Oborník M, Lukeš J. Make it, take it, or leave It: Heme metabolism of parasites. PLoS Pathog. 2013;9(1):e1003088. pmid: 23349629.
7. Oliveira MF, Silva JR, Dansa-Petretski M, de Souza W, Lins U, Braga CMS, et al. Haem detoxification by an insect. Nature. 1999;400(6744):517–8 pmid: 10448851.
8. Pijuan J, Moreno DF, Yahya G, Moisa M, Ul Haq I, Krukiewicz K, et al. Regulatory and pathogenic mechanisms in response to iron deficiency and excess in fungi. Microb Biotechnol. 2023;16(11):2053–71 pmid: 37804207.
9. Egan TJ, Combrinck JM, Egan J, Hearne GR, Marques HM, Ntenteni S, et al. Fate of haem iron in the malaria parasite *Plasmodium falciparum*. Biochem J. 2002;365(pt 2):343–7 pmid: 12033986.
10. Lara FA, Lins U, Paiva-Silva G, Almeida IC, Braga CM, Miguens FC, et al. A new intracellular pathway of haem detoxification in the midgut of the cattle tick *Boophilus microplus*: aggregation inside a specialized organelle, the hemosome. J Exp Biol. 2003;206(pt 10):1707–15 pmid: 12682102.
11. Niles JC, DeRisi JL, Marletta MA. Inhibiting *Plasmodium falciparum* growth and heme detoxification pathway using heme-binding DNA aptamers. Proc Natl Acad Sci U S A. 2009;106(32):13266–71 pmid: 19633187.
12. Matz JM. *Plasmodium*'s bottomless pit: properties and functions of the malaria parasite's digestive vacuole. Trends Parasitol. 2022;38(7):525–43 pmid: 35317985.
13. Lisewski AM. *Plasmodium* spp. membrane glutathione S-transferases: detoxification units and drug targets. Microb Cell. 2014;1(11):387–9 pmid: 28357217.
14. Lisewski AM, Quiros JP, Ng CL, Adikesavan AK, Miura K, Putluri N, et al. Supergenomic network compression and the discovery of EXP1 as a glutathione transferase inhibited by artesunate. Cell. 2014;158(4):916–28 pmid: 25126794.
15. Perner J, Gasser RB, Oliveira PL, Kopáček P. Haem biology in metazoan parasites – "The Bright Side of Haem." Trends Parasitol. 2019;35(3):213–25. https://doi.org/10.1016/j.pt.2019.01.001. pmid:30686614.
16. Rao AU, Carta LK, Lesuisse E, Hamza I. Lack of heme synthesis in a free-living eukaryote. Proc Natl Acad Sci U S A. 2005;102(12):4270–5 pmid: 15767563.
17. Chen C, Samuel TK, Sinclair J, Dailey HA, Hamza I. An intercellular heme trafficking protein delivers maternal heme to the embryo during development in *C. elegans*. Cell. 2011;145(5):720–31 pmid: 21620137.
18. Chen C, Samuel TK, Krause M, Dailey HA, Hamza I. Heme utilization in the *Caenorhabditis elegans* hypodermal cells is facilitated by heme-responsive gene-2. J Biol Chem. 2012;287(12):9601–12 pmid: 22303006.
19. Korolnek T, Zhang J, Beardsley S, Scheffer GL, Hamza I. Control of metazoan heme homeostasis by a conserved multidrug resistance protein. Cell Metab. 2014;19(6):1008–19 pmid: 24836561.
20. Rajagopal A, Rao AU, Amigo J, Tian M, Upadhyay SK, Hall C, et al. Haem homeostasis is regulated by the conserved and concerted functions of HRG-1 proteins. Nature. 2008;453(7198):1127–31 pmid: 18418376.
21. Sinclair J, Pinter K, Samuel T, Beardsley S, Yuan X, Zhang J, et al. Inter-organ signaling by HRG-7 promotes systemic heme homeostasis. Nat Cell Biol. 2017;19(7):799–807 pmid: 28581477.
22. Sun F, Zhao Z, Willoughby MM, Shen S, Zhou Y, Shao Y, et al. HRG-9 homologues regulate haem trafficking from haem-enriched compartments. Nature. 2022;610(7933):768–74 pmid: 36261532.
23. Yuan X, Protchenko O, Philpott CC, Hamza I. Topologically conserved residues direct heme transport in hrg-1-related proteins. J Biol Chem. 2012;287(7):4914–24 pmid: 22174408.
24. Chen AJ, Yuan X, Li J, Dong P, Hamza I, Cheng J-X. Label-free imaging of heme dynamics in living organisms by transient absorption microscopy. Anal Chem. 2018;90(5):3395–401 pmid: 29401392.
25. Chen C, Hamza I. Notes from the underground: Heme homeostasis in *C elegans*. Biomolecules. 2023;13(7):1149 pmid: 37509184.
26. Zhou J-R, Bu D-R, Zhao X-F, Wu F, Chen X-Q, Shi H-Z, et al. *Hc-hrg-2*, a glutathione transferase gene, regulates heme homeostasis in the blood-feeding parasitic nematode *Haemonchus contortus*. Parasit Vectors. 2020;13(1):40 pmid: 31996262.
27. Yang Y, Zhou J, Wu F, Tong D, Chen X, Jiang S, et al. Haem transporter HRG-1 is essential in the barber's pole worm and an intervention target candidate. PLoS Pathog. 2023;19(1):e1011129 pmid: 36716341.
28. Bouchery T, Filbey K, Shepherd A, Chandler J, Patel D, Schmidt A, et al. A novel blood-feeding detoxification pathway in *Nippostrongylus brasiliensis* L3 reveals a potential checkpoint for arresting hookworm development. PLoS Pathog. 2018;14(3):e1006931 pmid: 29566094.
29. Liu L, Zhang Z, Liu H, Zhu S, Zhou T, Wang C, et al. Identification and characterisation of the haemozoin of *Haemonchus contortus*. Parasit Vectors. 2023;16(1):88 pmid: 36879311.
30. Luck AN, Yuan X, Voronin D, Slatko BE, Hamza I, Foster JM. Heme acquisition in the parasitic filarial nematode *Brugia malayi*. FASEB J. 2016;30(10):3501–14 pmid: 27363426.
31. Wang Z, Zeng P, Zhou B. Identification and characterization of a heme exporter from the MRP family in *Drosophila melanogaster*. BMC Biol. 2022;20(2):126 pmid: 35655259.
32. Laing R, Kikuchi T, Martinelli A, Tsai IJ, Beech RN, Redman E, et al. The genome and transcriptome of *Haemonchus contortus*, a key model parasite for drug and vaccine discovery. Genome Biol. 2013;14(8):R88 pmid: 23985316.
33. Leite DFP, Echevarria-Lima J, Calixto JB, Rumjanek VM. Multidrug resistance related protein (ABCC1) and its role on nitrite production by the murine macrophage cell line RAW 264.7. Biochem Pharmacol. 2007;73(5):665–74 pmid: 17169333.
34. Worthington MT, Cohn SM, Miller SK, Luo RQ, Berg CL. Characterization of a human plasma membrane heme transporter in intestinal and hepatocyte cell lines. Am J Physiol Gastrointest Liver Physiol. 2001;280(6):G1172–7 pmid: 11352810.
35. Crisp RJ, Pollington A, Galea C, Jaron S, Yamaguchi-Iwai Y, Kaplan J. Inhibition of heme biosynthesis prevents transcription of iron uptake genes in *yeast*. J Biol Chem. 2003;278(46):45499–506 pmid: 12928433.
36. Protchenko O, Shakoury-Elizeh M, Keane P, Storey J, Androphy R, Philpott CC. Role of pug1 in inducible porphyrin and heme transport in *Saccharomyces cerevisiae*. Eukaryot Cell. 2008;7(5):859–71 pmid: 18326586.
37. van Rossum AJ, Jefferies JR, Rijsewijk FAM, LaCourse EJ, Teesdale-Spittle P, Barrett J, et al. Binding of hematin by a new class of glutathione transferase from the blood-feeding parasitic nematode *Haemonchus contortus*. Infect Immun. 2004;72(5):2780–90 pmid: 15102788.
38. Ma G, Wang T, Korhonen PK, Young ND, Nie S, Ang C-S, et al. Dafachronic acid promotes larval development in *Haemonchus contortus* by modulating dauer signalling and lipid metabolism. PLoS Pathog. 2019;15(7):e1007960 pmid: 31335899.
39. Sinclair J, Hamza I. A novel heme-responsive element mediates transcriptional regulation in *Caenorhabditis elegans*. J Biol Chem. 2010;285(50):39536–43 pmid: 20938051.
40. Blaxter M, Koutsovoulos G. The evolution of parasitism in Nematoda. Parasitology. 2015;142:S26–39 pmid: 24963797.
41. James CE, Davey MW. Increased expression of ABC transport proteins is associated with ivermectin resistance in the model nematode *Caenorhabditis elegans*. Int J Parasitol. 2009;39(2):213–20 pmid: 18708066.
42. Mladineo I, Trumbić Ž, Hrabar J, Vrbatović A, Bušelić I, Ujević I, et al. Efficiency of target larvicides is conditioned by abc-mediated transport in the zoonotic nematode *Anisakis pegreffii*. Antimicrob Agents Chemother. 2018;62(9):e00916-18 pmid: 29987147.
43. Raza A, Kopp SR, Bagnall NH, Jabbar A, Kotze AC. Effects of *in vitro* exposure to ivermectin and levamisole on the expression patterns of ABC transporters in *Haemonchus contortus* larvae. Int J Parasitol Drugs Drug Resist. 2016;6(2):103–15 pmid: 27164439.
44. Tompkins JB, Stitt LE, Morrissette AM, Ardelli BF. The role of *Brugia malayi* ATP-binding cassette (ABC) transporters in potentiating drug sensitivity. Parasitol Res. 2011;109(5):1311–22 pmid: 21494842.

45. Mangelsdorf DJ, Thummel C, Beato M, Herrlich P, Schütz G, Umesono K, et al. The nuclear receptor superfamily: The second decade. Cell. 1995;83(6):835–9 pmid: 8521507.
46. Wurtz JM, Bourguet W, Renaud JP, Vivat V, Chambon P, Moras D, et al. A canonical structure for the ligand-binding domain of nuclear receptors. Nat Struct Biol. 1996;3(2):206 pmid: 8564548.
47. Evans RM, Mangelsdorf DJ. Nuclear receptors. RXR & the Big Bang Cell. 2014;157:255–66 pmid: 24679540.
48. Antebi A, Yeh W-H, Tait D, Hedgecock EM, Riddle DL. *daf-12* encodes a nuclear receptor that regulates the dauer diapause and developmental age in *C elegans*. Genes Dev. 2000;14(12):1512–27 pmid: 10859169.
49. Motola DL, Cummins CL, Rottiers V, Sharma KK, Li T, Li Y, et al. Identification of ligands for daf-12 that govern dauer formation and reproduction in *C. elegans*. Cell. 2006;124(6):1209–23 pmid: 16529801.
50. Matyash V, Entchev EV, Mende F, Wilsch-Bräuninger M, Thiele C, Schmidt AW, et al. Sterol-derived hormone(s) controls entry into diapause in *Caenorhabditis elegans* by consecutive activation of DAF-12 and DAF-16. PLoS Biol. 2004;2(10). pmid: 15383841.
51. Ayoade KO, Carranza FR, Cho WH, Wang Z, Kliewer SA, Mangelsdorf DJ, et al. Dafachronic acid and temperature regulate canonical dauer pathways during *Nippostrongylus brasiliensis* infectious larvae activation. Parasit Vectors. 2020;13(1):162 pmid: 32238181.
52. Bétous R, Emile A, Che H, Guchen E, Concordet D, Long T, et al. Filarial DAF-12 sense the host serum to resume iL3 development during infection. PLoS Pathog. 2023;19(6):e1011462 pmid: 37339136.
53. Rajan M, Anderson CP, Rindler PM, Romney SJ, Ferreira dos Santos MC, Gertz J, et al. NHR-14 loss of function couples intestinal iron uptake with innate immunity in *C. elegans* through PQM-1 signaling. Elife. 2019;8:e44674 pmid: 31532389.
54. Sang L, Dong R, Liu R, Hao Q, Bai W, Sun J. *Caenorhabditis elegans* NHR-14/HNF4α regulates DNA damage-induced apoptosis through cooperating with cep-1/p53. Cell Commun Signal. 2022;20(1):135 pmid: 36050770.
55. Ménez C, Alberich M, Courtot E, Guegnard F, Blanchard A, Aguilaniu H, et al. The transcription factor NHR-8: A new target to increase ivermectin efficacy in nematodes. PLoS Pathog. 2019;15(2):7598 pmid: 30759156.
56. Ma G, Wang T, Korhonen PK, Ang C-S, Williamson NA, Young ND, et al. Molecular alterations during larval development of *Haemonchus contortus in vitro* are under tight post-transcriptional control. Int J Parasitol. 2018;48(9–10):763–72 pmid: 29792880.
57. International Helminth Genomes Consortium. Comparative genomics of the major parasitic worms. Nat Genet. 2019;51(1):163–74 pmid: 30397333.
58. Jones P, Binns D, Chang H-Y, Fraser M, Li W, McAnulla C, et al. InterProScan 5: genome-scale protein function classification. Bioinformatics. 2014;30(9):1236–40 pmid: 24451626.
59. Kumar S, Stecher G, Li M, Knyaz C, Tamura K. MEGA X: Molecular evolutionary genetics analysis across computing platforms. Mol Biol Evol. 2018;35(6):1547–9 pmid: 29722887.
60. Schwarz EM, Korhonen PK, Campbell BE, Young ND, Jex AR, Jabbar A, et al. The genome and developmental transcriptome of the strongylid nematode *Haemonchus contortus*. Genome Biol. 2013;14(8):R89 pmid: 23985341.60.
61. Doyle SR, Tracey A, Laing R, Holroyd N, Bartley D, Bazant W, et al. Genomic and transcriptomic variation defines the chromosome-scale assembly of *Haemonchus contortus*, a model gastrointestinal worm. Commun Biol. 2020;3(1):656 pmid: 33168940.61.
62. Li B, Dewey CN. RSEM: accurate transcript quantification from RNA-Seq data with or without a reference genome. BMC Bioinformatics. 2011;12:323 pmid: 21816040.
63. Langmead B, Salzberg SL. Fast gapped-read alignment with Bowtie 2. Nat Methods. 2012;9(4):357–9 pmid: 22388286.
64. Huang Y, Wu J, Chen X, Tong D, Zhou J, Wu F, et al. A zinc metalloprotease *nas-33* is required for molting and survival in parasitic nematode *Haemonchus contortus*. Front Cell Dev Biol. 2021;9:695003. pmid: 34327203.
65. Ke D, Ménard C, Picard FJ, Boissinot M, Ouellette M, Roy PH, et al. Development of conventional and real-time PCR assays for the rapid detection of group B streptococci. Clin Chem. 2000;46:324–31 pmid: 10702518.
66. Campeau E, Ruhl VE, Rodier F, Smith CL, Rahmberg BL, Fuss JO, et al. A versatile viral system for expression and depletion of proteins in mammalian cells. PLoS One. 2009;4(8):e6529. pmid: 19657394.
67. Dogan AL, Legrand O, Faussat A-M, Perrot J-Y, Marie J-P. Evaluation and comparison of MRP1 activity with three fluorescent dyes and three modulators in leukemic cell lines. Leuk Res. 2004;28(6):619–22 pmid: 15120939.
68. Burke D, Dawson D, Sterns T. Methods in *yeast* genetics: a Cold Spring Harbor Laboratory course manual. 2000 ed. Tsinghua University Press; c2002.
69. Ito H, Fukuda Y, Murata K, Kimura A. Transformation of intact *yeast* cells treated with alkali cations. J Bacteriol. 1983;153(1):163–8 pmid: 6336730.
70. Zawadzki JL, Kotze AC, Fritz J-A, Johnson NM, Hemsworth JE, Hines BM, et al. Silencing of essential genes by RNA interference in *Haemonchus contortus*. Parasitology. 2012;139(5):613–29 pmid: 22348596.
71. He L, Gasser RB, Korhonen PK, Di W, Li F, Zhang H, et al. A TGF-β type I receptor-like molecule with a key functional role in *Haemonchus contortus* development. Int J Parasitol. 2018;48(13):1023–33 pmid: 30266591.
72. Sato H, Kusel JR, Thornhill J. Excretion of fluorescent substrates of mammalian multidrug resistance-associated protein (MRP) in the *Schistosoma mansoni* excretory system. Parasitology. 2004;128(pt 1):43–52 pmid: 15002903.
73. Dulovic A, Streit A. RNAi-mediated knockdown of *daf-12* in the model parasitic nematode *Strongyloides ratti*. PLoS Pathog. 2019;15(3):e1007705. pmid: 30925161.
74. Khan S, Nisar A, Yuan J, Luo X, Dou X, Liu F, et al. A whole genome re-sequencing based gwa analysis reveals candidate genes associated with ivermectin resistance in *Haemonchus contortus*. Genes (Basel). 2020;11(4):367 pmid: 32231078.
75. Sun J, Hu W, Li C. Beyond heme detoxification: a role for hemozoin in iron transport in *S. japonicum*. Parasitol Res. 2013;112(8):2983–90 pmid: 23733233.
76. Preston S, Jabbar A, Nowell C, Joachim A, Ruttkowski B, Baell J, et al. Low cost whole-organism screening of compounds for anthelmintic activity. Int J Parasitol. 2015;45(5):333–43 pmid: 25746136.
77. Xu X, Zhang N, Meng X, Jiang H, Ge H, Zheng Y, et al. FOXO acts as a positive regulator of CncC and deltamethrin tolerance in the red flour beetle, *Tribolium castaneum*. Pest Manag Sci. 2022;78(5):1938–45 pmid: 35085425.

Publisher's Note